Numerical analysis on effects of high dielectric material with 4-channel phase array

Wei Luo[1], Giuseppe Carluccio[2,3], Sukhoon Oh[3], and Christopher M Collins[3]

[1]*Department of Engineering Science and Mechanics, The Pennsylvania State University, University Park, PA, United States,* [2]*Department of Electrical and Computer Engineering, University of Illinois at Chicago, Chicago, IL, United States,* [3]*Radiology, The Pennsylvania State University, Hershey, PA, United States*

Introduction: The effects of high dielectric material (HDM) in human MRI have been studied intensively in recent years. Promising enhancements on transmit EM field and local SNR have been shown in experiments from different groups with different HDMs [1,2]. An effort to understand the effect of HDM has been ongoing, but has mainly focused on the aspect of the transmit EM field. In this study, we consider both transmit fields from a body coil and receive fields for a 4-channel receive array. The knowledge of the effect of HDM on the receive EM field will provide us a complete picture of overall behavior of HDM in human MRI, providing better insight to use of HDM for maximum performance of MRI.

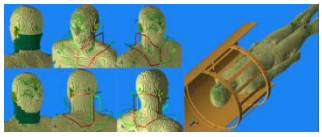

Figure 1: Model used in simulation. Dark green indicates dielectric pad. Elements of 4-channel receive array are shown in different colors. Body coil and part of shield are shown on right.

Methods: A 75-tissue human model ("Duke") at 5mm^3 resolution with electrical properties of tissues at f =123.26MHz was used in this simulation [3]. HDM was placed around the neck area (2 cm thick) with a dielectric constant of 515 and conductivity of 0.35 S/m. The transverse EM field was excited by a copper 16-element birdcage coil (62 cm diameter, 48 cm length, and 68 cm shield length) with unit current source (having phase appropriate to simulate ideal mode 1 resonance) placed in the middle of each end ring segment. A 4-loop phase array was modeled based on a commercial neck coil, with unit current sources placed at capacitor gaps in simulation to calculate the receive sensitivity distribution. The simulation model is shown in Figure 1. The transmit sensitivity map ($|B_1^+|$) and receive sensitivity map were calculated from the lager circularly-polarized component of the EM field generated by the birdcage coil and each individual loop in the receive array separately [5]. The magnitude combined receive sensitivity (B_1^-[Mag Comb]) was later calculated as described in [4]. Voxel-based intrinsic SNR was obtained by $iSNR = M_0\omega \sin(V|B_1^+|\tau\gamma) \cdot (B_1^-[\text{Mag Comb}]) \cdot dv/\sqrt{4kTdf}$, where normalization factor V (proportional to driving voltage)was determined so that the amplitude of the total signal from the axial slice is maximized for a rectangular excitation pulse with a duration (τ) of 3 ms. The SAR in each voxel was calculated to generate the normalized 10 gram SAR ($V^2\text{SAR}_{10g}$) [5]. All field computations were performed with finite difference time domain numerical method using commercially available software (XFDTD; Remcom Inc, State College, PA) and post processing of the EM fields was done using Matlab (The Mathworks, Natick, MA).

	With Pad [W/kg]	Without Pad [W/kg]
V	21.4302	28.2195
V^2 Avg SAR (Whole Body)	4.4548	7.3263
Max $V^2\text{SAR}_{10g}$ (Sagittal)	183.8308	292.9743
Avg $V^2\text{SAR}_{10g}$ (Axial)	12.9433	20.0516

Results: In Figure 2, data on an axial slice and a sagittal slice for various quantities calculated with and without the dielectric pad in place are plotted. The magnitude of the pertinent circularly-polarized component of the EM field ($|B_1^+|_{\text{norm}}$) produced by the birdcage coil was normalized by the dissipated power in tissue and is shown in Figure 2 (a). The magnitude-combined receive sensitivity of the phase array was calculated as presented in Roemer et al and it is shown in Figure 2 (b). The percentage increase of the $|B_1^+|_{\text{norm}}$ between the data with and without HDM present is shown in the left column of Figure 2 (d). The percentage increase of the *i*SNR data is shown in the right column of Figure 2 (d). The percentage increase for a given value Val was calculated as $(Val[\text{Pad}] - Val[\text{NoPad}])/Val[\text{NoPad}] \times 100\%$. Figure 2 (c) and (e) show the intrinsic SNR data and the normalized 10 gram SAR data for both axial and sagittal slices. Normalization factor V, average SAR for whole body, and the maximum and average $V^2\text{SAR}_{10g}$ for both sets of data are shown in the table.

Discussion: When the HDM is present, the $|B_1^+|_{\text{norm}}$ data in Figure 2 (a) shows a significant increase within the corresponding neck region in both axial and sagittal slices. The HDM appears to enhance the $|B_1^+|_{\text{norm}}$ in the neck. This can been observed clearly in the sagittal slice of $|B_1^+|_{\text{norm}}$ and the percentage increase of the $|B_1^+|_{\text{norm}}$ in the left column of Figure 2 (d). The percentage increase of the $|B_1^+|_{\text{norm}}$ in the axial slice 11.1% on average. Because of this, the power required to achieve a given flip angle in the neck region is lower and the normalization factor V (proportional to driving voltage) is smaller when the HDM is present. For this particular study, the normalization factor V was 21.4302 and 28.2195 when HDM is present and absent respectively. Figure 2 (b) also shows an increase of B_1^-[Mag Comb] in the neck region when the HDM is present in both slices. Even though B_1^-[Mag Comb] is not an optimized receive sensitivity, an increase of B_1^-[Mag Comb]is still observed. Where values of B_1^-[Mag Comb] increase when HDM is present, as we expect, the values of *i*SNR are higher when the HDM is present in both the axial and sagittal slices as shown in Figure 2 (c). Since the receive sensitivity was not optimized, the values of percentage increase are not as pronounced as they might be. Indeed, in experiments with a dielectric pad and receive array much like those simulated here [6], SNR increases were seen to be somewhat greater and further-reaching than those shown here. Still, this work illustrates that with HDM enhancement of the transmit RF field in the region of interest, lower SAR levels can be achieved, and with HDM enhancement of receive RF fields in the region of interest. The improvement of SNR with HDM is simulated here for the first time in a receive array, and it is now clear that it does not have to be relate to improved excitation or local enhancement of fields of a volume coil, as has been understood previously.

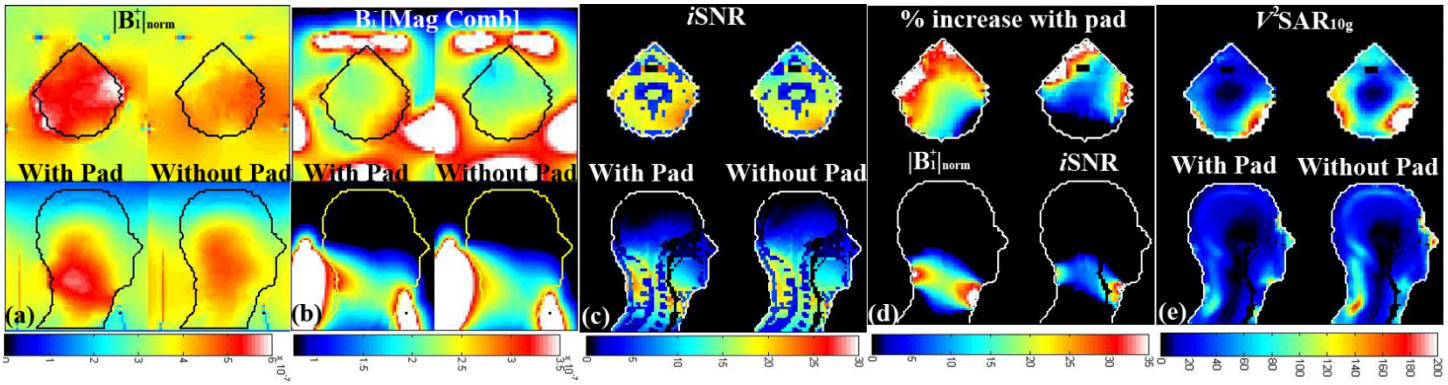

Figure 2: (a) Normalized transmit sensitivity ($|B_1^+|_{\text{norm}}$) map. (b) Magnitude combined receive sensitivity (B_1^-[Mag Comb]) map. (c)intrinsic SNR (*i*SNR) map (d) Percentage increase of $|B_1^+|_{\text{norm}}$ (left column) and *i*SNR (left column). (d) Normalized 10 gram SAR ($V^2\text{SAR}_{10g}$) map.

Reference: (**1**) Haines K., et al. JMR 2010. 203:323-327. (**2**) Yang QX, et al. JMRI 2006. 24:197-202 (**3**) Christ A, et al. Phys Med Biol 2010. 55:N23-N38 (**4**) Roemer PB, et al. MRM 1990. 16:192-225 (**5**) Collins CM, et al. MRM 2001. 45:684-691 (**6**) Yang QX et al., Proc 2011 ISMRM, p. 621

Acknowledgements: Funding for this work was provided by the NIH.